INTERNATIONAL JOURNAL FOR NUMERICAL METHODS IN FLUIDS
Int. J. Numer. Meth. Fluids **29**: 363–371 (1999)

CONVERGED SOLUTIONS OF THE NEWTONIAN EXTRUDATE-SWELL PROBLEM

GEORGIOS C. GEORGIOU[a,*] AND ANDREAS G. BOUDOUVIS[b]

[a] *Department of Mathematics and Statistics, University of Cyprus, Kallipoleos 75, P.O. Box 537, 1678 Nicosia, Cyprus*
[b] *Department of Chemical Engineering, National Technical University of Athens, Zografou Campus, Athens 15780, Greece*

SUMMARY

Both the axisymmetric and the planar Newtonian extrudate-swell problems are solved using the standard and the singular finite element methods. In the latter method, special elements that incorporate the radial form of the stress singularity are used around the exit of the die. The convergence of each of the two methods with mesh refinement is studied for various values of the Reynolds and the capillary numbers. The numerical results show that the singular finite elements perform well if coarse or moderately refined meshes are used, and appear to be superior to the standard finite elements only when the Reynolds number is low and the surface tension is not large. The standard finite elements perform better as the surface tension or the Reynolds number are increased. This implies that the effect of the stress singularity on the accuracy of the numerical solution in the neighborhood of the die exit becomes less significant when the Reynolds number is high or the surface tension is large. Copyright © 1999 John Wiley & Sons, Ltd.

KEY WORDS: extrudate-swell; singular finite elements; convergence

1. INTRODUCTION

In this paper, the singular finite element method (SFEM), developed by Georgiou *et al.* [1,2] for solving Newtonian flow problems with boundary stress singularities is revisited. In the SFEM, special elements incorporating the radial form of the local solution by means of singular basis functions are employed in a small region around the singularity, while standard elements are used in the rest of the domain. The basic motive behind using singular methods is to improve the accuracy and the rate of convergence of the solution with mesh refinement, which are rather unsatisfactory with standard numerical methods, especially in the neighborhood of the singularity. The poor performance of the standard FEM is attributed to the fact that the calculated pressure and stresses cannot be infinite at the singular point, as required by the local asymptotic solution, and are thus tainted by spurious oscillations. This difficulty is overcome with the SFEM.

Georgiou *et al.* [2] applied the SFEM to the planar Newtonian extrudate-swell problem, which describes the extrusion of a viscous fluid through a die into an inviscid medium. This is a well-known free-surface problem; at low Reynolds numbers, the fluid swells as it comes out

* Correspondence to: Department of Mathematics and Statistics, University of Cyprus, Kallipoleos 75, P.O. Box 537, 1678 Nicosia, Cyprus.

CCC 0271–2091/99/030363–09$17.50

Received 14 August 1997
Revised 3 March 1998

of the die. Another important characteristic of this flow is the presence of a stress singularity at the exit of the die, resulting from the sudden change in the boundary condition from the wall of the die to the free-surface of the extrudate. The singular finite element calculations for the planar Newtonian extrudate-swell problem have revealed that the spurious stress oscillations that characterize the stresses in the standard finite element solution are eliminated, and that the convergence of the free surface profile with mesh refinement is considerably accelerated [2]. The SFEM is not free of drawbacks [1]. Firstly, extensive mesh refinement is not possible with the SFEM. As the mesh is refined, the singular elements become smaller in size, and consequently, the size of the region over which the singularity is given special attention is reduced. Second, the method can be implemented only if the radial form of the local solution is known, at least approximately. This implies that the method is not applicable to many important problems, such as most visco-elastic flow problems in which the inaccuracies, stemming from the failure to satisfactorily approximate the stress behavior near the singularity, are in general, more severe.

In this paper, the round and planar Newtonian extrudate-swell problems are solved using both the standard and the SFE methods. The convergence of the numerical solutions with mesh refinement is systematically studied. The objective is to compare the performance of the two methods and to obtain accurate estimates of the position of the free-surface and the extrudate-swell ratio. These results can be quite useful in testing other numerical methods proposed in the literature. In Section 2, the governing equations and the boundary conditions for the axisymmetric extrudate-swell problem are briefly presented, and the assumptions made for the construction of the singular basis functions are discussed. In Section 3, the finite element formulation is outlined. The numerical results are presented and discussed in Section 4. Comparisons are made with the standard finite element results for various values of the Reynolds number and the capillary number (the ratio of viscous to surface tension forces). The numerical calculations reveal that the singular finite elements accelerate the convergence of the free-surface when the Reynolds number is low and the surface tension is not high.

2. GOVERNING EQUATIONS

The flow geometry and the dimensionless governing equations and boundary conditions for the steady state, axisymmetric, incompressible extrudate-swell problem are depicted in Figure

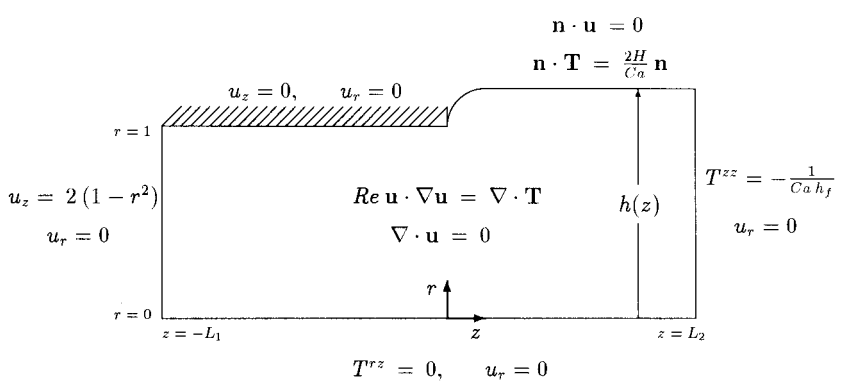

Figure 1. Geometry and boundary conditions for the extrudate-swell problem.

Table I. Data for ordinary element meshes ($L_2 = 20$)

Mesh	Number of elements	Number of nodes	Degrees of freedom	Size of corner elements
OM1	140	639	1506	0.2
OM2	276	1209	2807	0.1
OM3	472	2023	4660	0.05
OM4	781	3289	7528	0.025
OM5	1335	5549	12 642	0.01
OM6	1818	7511	17 076	0.005
OM7	3325	13 617	30 866	0.0025

1. The scaling parameter for lengths is either the radius R or the channel half-width, for the axisymmetric and planar problems respectively. The velocity vector $\boldsymbol{u}$ is scaled by the mean velocity U, and finally, the pressure p and the stress tensor $\boldsymbol{T}$ are measured in units of $\eta U/R$, where η is the viscosity. This non-dimensionalization yields two dimensionless numbers, the Reynolds number,

$$Re \equiv \frac{\rho U R}{\eta}, \tag{1}$$

where ρ is the density, and the capillary number,

$$Ca \equiv \frac{\eta U}{\sigma}, \tag{2}$$

where σ is the surface tension. The governing equations and the boundary conditions are described in detail elsewhere [2].

A prerequisite for the construction of the singular finite elements is the knowledge of the radial form of the singularity. Assuming that the slope of the free-surface at the singular point is zero, one can show that, in the plane flow, the velocity components vary as

$$u_x \ (\text{or } u_y) \approx A_1 r^{1/2} + A_2 r + A_3 r^{3/2} + A_4 r^2 + \cdots, \tag{3}$$

while the pressure varies as

$$p \approx B_1 r^{-1/2} + B_2 + B_3 r^{1/2} + B_4 r + \cdots, \tag{4}$$

where r is the radial distance from the singular point, and A_i and B_i are constants. The latter assumption is based on Michael's analysis for vanishingly small surface tension on a planar free-surface [3], and eliminates the need of finding the angle of separation and constructing appropriate singular basis functions [2]. In fact, Georgiou *et al.* [2] showed that the numerical results are not sensitive to small variations of the singularity powers used for the planar extrudate-swell problem. Their results are consistent with the numerical results of Salamon *et al.* [4] for finite capillary numbers, which reveal that the values of λ are in the range $1.50 \ll \lambda \ll 1.55$ and correspond to singular, albeit integrable, stresses. Georgiou *et al.* [2] obtained accurate oscillation-free results with rather coarse meshes, not only for the limiting case of zero Reynolds number and zero surface tension but also for small and moderate values of the Reynolds number, and for a wide range of capillary numbers. Using the SFEM for non-zero Reynolds number flows is justified by the fact that the local solution remains unchanged around the singular point where viscous effects dominate. Moreover, as surface tension increases, the flow approaches the stick–slip flow limit, the local solution of which was used for designing the singular elements.

Table II. Data for singular element meshes ($L_2 = 20$)

Mesh	Number of elements	Number of nodes	Degrees of freedom	Radius of corner elements
SM1	148	697	1654	0.24
SM2	284	1267	2955	0.12
SM3	480	2061	4808	0.06
SM4	789	3347	7676	0.03
SM5	1343	5607	12 790	0.012
SM6	1826	7569	17 224	0.006
SM7	3333	13 675	31 034	0.003

Although the analysis of Michael [3] does not apply to the axisymmetric extrudate-swell problem, the same elements will be used for solving the axisymmetric extrudate-swell problem. In fact, the analytical solution for the axisymmetric stick–slip problem obtained by Sturges [5] reveals that the velocity components u_z and u_r follow Equations (3) and (4) respectively. Thus, it is reasonable to assume that the radial form of the singularity in the axisymmetric extrudate-swell problem is the same. It will be verified, in Section 4, that the accuracy and the rate of convergence achieved with the singular elements are quite satisfactory.

3. FINITE ELEMENT FORMULATION

The flow domain is discretized by means of eight singular elements around the singular point and standard rectangular elements elsewhere. Let $\mathbf{\Phi}^i$ and $\mathbf{\Psi}^i$ denote the basis functions used for the finite element approximations of the velocity vector and the pressure respectively. Over the ordinary elements, $\mathbf{\Phi}^i$ are biquadratic ($P^2 - C^0$) and $\mathbf{\Psi}^i$ are bilinear ($P^1 - C^0$). (These are the most common approximations used for Newtonian flow.) The ordinary elements thus contain nine velocity and four pressure nodes. The singular elements are collapsed quadrilaterals with 13 velocity nodes and eight pressure nodes. In contrast to the polynomial basis functions used with ordinary elements, the basis functions for $\boldsymbol{u}$ and p over the singular elements are constructed so that they embody the behavior of the leading four terms of Equations (3) and (4) respectively, in the radial direction. Towards this end, it is very convenient to have

Table III. Calculated extrudate-swell ratios for the round and the planar jets at $Re = 0$ and zero surface tension ($L_2 = 5$)

Mesh	Round jet		Planar jet	
	Ordinary elements	Singular elements	Ordinary elements	Singular elements
1	1.1594	1.1260	1.2209	1.1859
2	1.1435	1.1263	1.2049	1.1862
3	1.1356	1.1265	1.1965	1.1863
4	1.1314	1.1265	1.1919	1.1863
5	1.1287	1.1265	1.1888	1.1863
6	1.1276	1.1264[a]	1.1876	1.1860[a]
7	1.1271	1.1260[a]	1.1869	Diverge

[a] The corresponding solutions are tainted by wiggles near the exit.

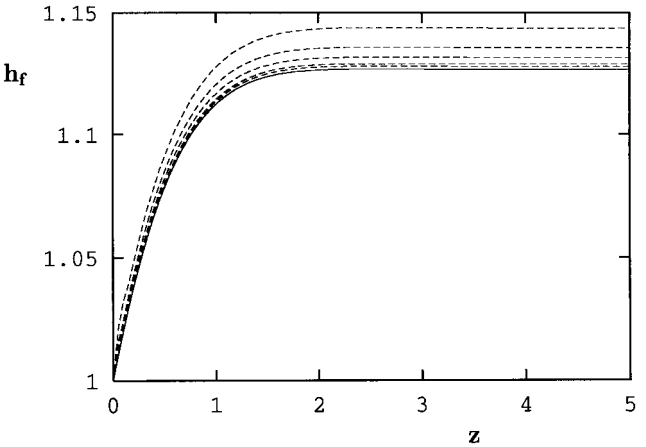

Figure 2. Free-surface profiles with ordinary element meshes OM1–OM5 (dashed lines) and SM1 (solid line); axisymmetric extrudate-swell problem, $Re = 0$ and $Ca = \infty$.

triangular, and not rectangular, singular elements with one vertex at the singular point. From Equation (4), it is also clear that the pressure is infinite at the singular point. This fact is taken care of by the singular basis functions; thus, no pressure node is placed at the singular point. In other words, the need to calculate an infinite quantity is eliminated. This is one of the most important features of the singular finite elements, resulting in the elimination of the Gibbs-type oscillations of the pressure. More details about the construction and the complete expressions of the basis functions for $\boldsymbol{u}$ and p may be found in [1]. Finally, to approximate the unknown position of the free-surface h, quadratic basis functions are used.

The standard Galerkin method is used to weight the momentum, the continuity and the kinematic equations. The resulting non-linear system of equations is solved using the Newton method and a standard frontal subroutine. The mesh is updated at each iteration by the newly found free-surface location values. The nodes of the singular elements are at a constant distance from the singular point, rotating around the singular point according to the shape and the position of the free surface [2]. The standard 3×3 and a modified 5×3 Gaussian quadratures are used for the numerical integration over the ordinary and the singular elements respectively [1].

4. RESULTS AND DISCUSSION

For the convergence studies, seven ordinary element meshes, OM1–OM7, were constructed. From them, the singular element meshes, SM1–SM7, were generated by replacing eight elements around the singular point by eight singular and eight ordinary elements. All meshes extended up to five radii upstream ($L_1 = 5$). Three different values were considered for the length L_2 of the domain downstream of the exit, i.e. $L_2 = 5$, 20 and 40. In Tables I and II, useful data about the ordinary and singular meshes with $L_2 = 20$ are tabulated.

Considered first was the creeping flow ($Re = 0$) with zero surface tension ($Ca = \infty$). For this particular case, the value $L_2 = 5$ for the length of the extrudate is adequate to capture the swelling of the extrudate. The numerical results obtained with the three values of L_2 are the same up to five significant digits. The values of the extrudate-swell ratios (h_f) calculated with

both the ordinary and singular elements are tabulated in Table III. As pointed out by Tanner [6], swelling is generally reduced as the number of degrees of freedom is increased (i.e. as the mesh is refined), when using ordinary elements. From Table III, it is observed that this is not the case when the singular finite elements are used. It is also observed that the singular element solution converges much faster than its ordinary element counterpart. This is illustrated in Figure 2, where the free-surface profiles calculated with meshes OM1–OM5 are compared with that obtained with the coarsest singular element mesh SM1. Comparing the values of h_f given in Table III, note that the solution obtained with SM1 is more accurate than that obtained with the finest ordinary element mesh OM7.

As already mentioned, the performance of the SFEM deteriorates when the singular elements are small. Indeed, with the last two singular meshes (SM6 and SM7), oscillations appear on the free-surface, as illustrated in Figure 3. The inaccuracies propagate downstream, and they thus affect the calculated value of h_f. Note also, that with more refined meshes, the SFEM diverges. It is concluded that the most accurate results are obtained with mesh SM5. Hence, the converged values of h_f for zero Re and zero surface tension are 1.1265 and 1.1863

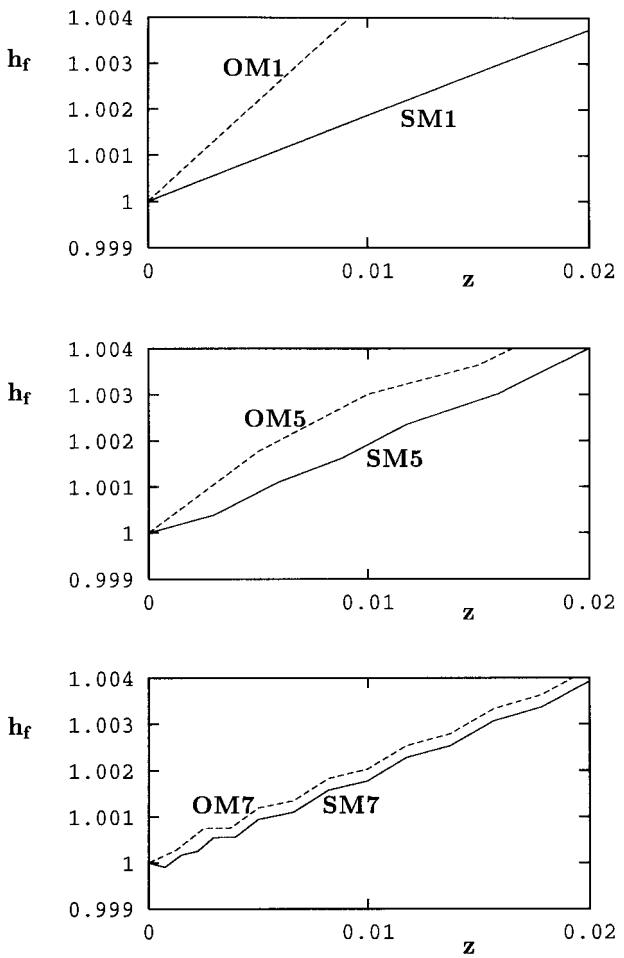

Figure 3. Free-surface profiles near the exit; axisymmetric extrudate-swell problem, $Re = 0$ and $Ca = \infty$.

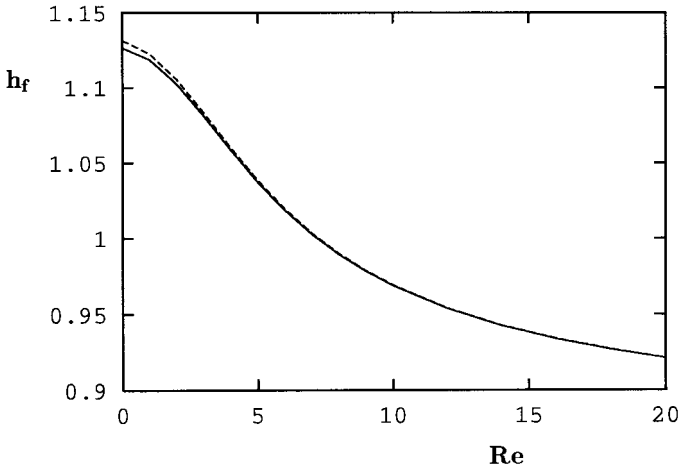

Figure 4. Calculated extrudate-swell ratios for the axisymmetric problem at zero surface tension ($Ca = \infty$); dashed line: standard finite elements, mesh OM4; solid line: singular finite elements, mesh SM4.

for the axisymmetric and planar problems respectively. Tanner [6] provided a selection of h_f values from the literature and estimated the extrapolated values $h_f = 1.127 \pm 0.003$ (axisymmetric) and $h_f = 1.190 \pm 0.002$ (plane) for an infinite number of degrees of freedom.

An interesting observation is that for $Re = 0$ (and any value of Ca), the free-surface is not a monotonic function of z (or x, in the planar flow). For $Ca = \infty$, the maximum is attained at a value of z in the interval (2.48, 2.60). No attempt has been made for calculating the exact location of the maximum since this is not particularly sharp ($h_{\max} \approx h_f + 0.0001$); such a calculation would have required extensive refinement in the direction of the flow. For lower values of Ca, the swelling is reduced and the maximum becomes less sharp. It is well-known that, as the Reynolds number is increased, the swelling of the extrudate is reduced and the jet actually contracts, above a critical value of Re [7]. In such a case, the free-surface is still non-monotonic and exhibits a minimum [7].

The performance of both the standard and the singular finite elements for Reynolds numbers ranging from 0 to 20 and for capillary numbers ranging from 0.01 to infinity has also been studied. A zero-order continuation was used for both Re and Ca, starting form $Re = 0$ and $Ca = \infty$. In the runs for non-zero Reynolds number, the longer meshes ($L_2 = 20$ and 40) were used. The results for both lengths were the same up to five significant digits. In Figure 4, results are shown for the axisymmetric extrudate-swell problem for zero surface tension ($Ca = \infty$). The extrudate-swell ratios calculated using meshes of moderate refinement, i.e. meshes OM4 and SM4, are plotted versus the Reynolds number. It is observed that the differences between the standard and the singular finite elements diminish as the Reynolds number is increased. This implies that the effect of the singularity on the free-surface profile becomes less severe at higher Reynolds number. Similar results have been obtained for the planar extrudate-swell problem.

In Figure 5, the convergence of the two methods for $Re = 0$ and various capillary numbers are presented for the case of the planar extrudate-swell problem. (The results for the axisymmetric problem are similar.) In Figure 5(a), the extrudate-swell ratios calculated with all standard meshes are plotted versus the capillary number. It is observed that, for $Ca < 1$, all meshes give practically the same results (up to four or five decimal digits). For higher values of the capillary number, the convergence of the standard FEM is rather slow. In Figure 5(b),

the extrudate-swell ratios calculated with all singular meshes are plotted. The singular finite elements give impressively accurate results, even with coarse meshes, for values of $Ca > 1$. For lower Ca values, the accuracy is not satisfactory. The method appears to converge slowly with mesh refinement. However, as the size of the singular elements is reduced, wiggles appear on the free-surface near the exit, which become more severe with meshes SM6 and SM7, and result in the divergence of the method. In Table IV, the best estimates from this study of the planar extrudate-swell ratios are given for various capillary numbers. The tabulated values for $Ca > 1$ have been obtained with the singular elements (mesh SM5), and the others with the ordinary elements (mesh OM7). The value 1.1291 for $Ca = 1$ agrees well with that calculated by Salamon *et al.* [4].

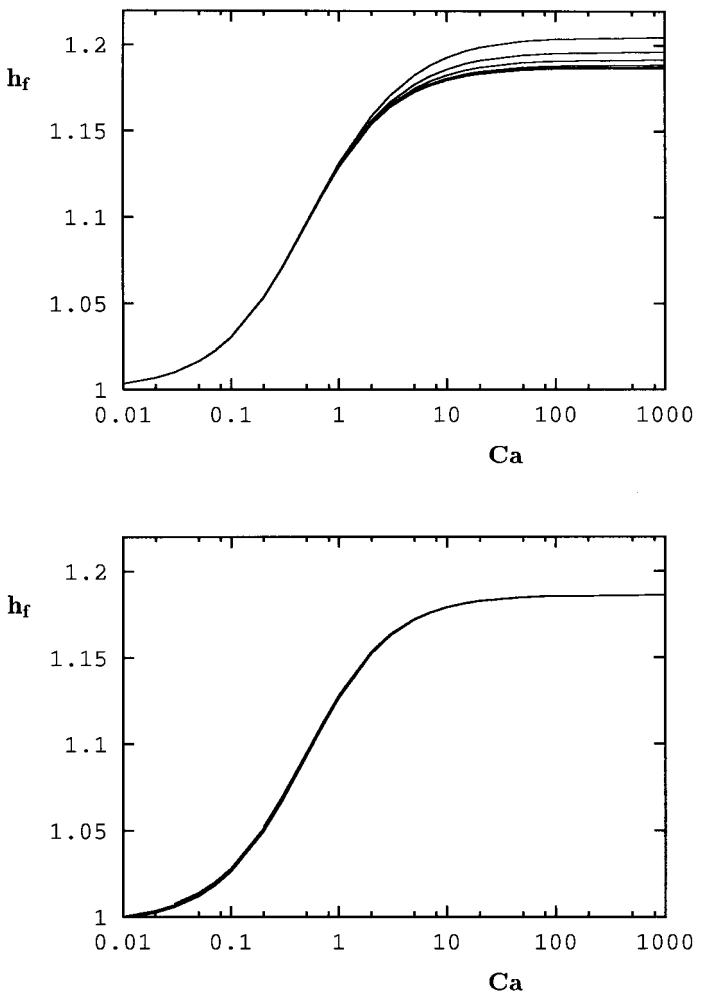

Figure 5. Calculated extrudate-swell ratios for the planar problem at zero *Re*: (a) standard finite elements, meshes OM2–OM7; (b) singular finite elements, meshes SM2–SM6.

Table IV. Calculated extrudate-swell ratios for the planar extrudate-swell problem at $Re = 0$

Ca	h_f
∞	1.1863
10	1.1794
5	1.1724
1	1.1291
0.5	1.0960
0.1	1.03047
0.05	1.01016
0.01	1.00350

5. CONCLUSIONS

The standard FEM and the SFEM have been applied to the planar and axisymmetric extrudate-swell problems. The convergence of the two methods with mesh refinement has been studied for various values of the Reynolds and the capillary numbers. It has been found that the singular finite elements accelerate the convergence of the free-surface when the Reynolds number is low and the surface tension is small. For high values of the surface tension and Reynolds number, the effect of the stress singularity on the numerical solution is less significant.

REFERENCES

1. G.C. Georgiou, L.G. Olson, W.W. Schultz and S. Sagan, 'A singular finite element for Stokes flow: the stick–slip problem', *Int. J. Numer. Methods Fluids*, **9**, 1353–1367 (1989).
2. G.C. Georgiou, L.G. Olson and W.W. Schultz, 'Singular finite elements for the sudden expansion and the die-swell problems', *Int. J. Numer. Methods Fluids*, **10**, 357–371 (1990).
3. D.H. Michael, 'The separation of a viscous liquid at a straight edge', *Mathematica*, **5**, 82–84 (1958).
4. T.R. Salamon, D.E. Bornside, R.C. Armstrong and R.A. Brown, 'The role of surface tension in the dominant balance in the die well singularity', *Phys. Fluids*, **7**, 2328 (1995).
5. L.D. Sturges, 'Die swell: the separation of the free surface', *J. Non-Newtonian Fluid Mech.*, **6**, 155–159 (1979).
6. R.I. Tanner, *Engineering Rheology*, Clarendon Press, Oxford, 1988.
7. G.C. Georgiou, T.C. Papanastasiou and J.O. Wilkes, 'Laminar jets at high Reynolds and high surface tension', *AIChE J.*, **24**, 1559–1562 (1988).

